

# Structural behavior of corroded RC beams with/without stirrups repaired with CFRP sheets

A. H. Al-Saidy · H. Saadatmanesh ·  
S. El-Gamal · K. S. Al-Jabri · B. M. Waris

Received: 24 March 2015 / Accepted: 23 November 2015 / Published online: 26 November 2015  
© RILEM 2015

**Abstract** Strengthening/repair of existing reinforced concrete structures has become one of the important issues in the field of civil engineering. In reinforced concrete structures located in hot and humid areas, steel reinforcement is generally vulnerable to deterioration due to corrosion. Corrosion of reinforcement in many cases is considered the main cause of concrete structures deterioration which in turn requires large budgets for repair and maintenance. This paper presents the experimental results of damaged/repared reinforced concrete beams. The experimental program consisted of testing 12 reinforced concrete rectangular beam specimens with/without shear reinforcement and exposed to accelerated corrosion. The corrosion level was varied between 5 and 7.5 % which represents mass loss of the longitudinal steel reinforcement on the tension side. Corroded beams without shear reinforcement were repaired by bonding longitudinal carbon fiber reinforced polymer (CFRP) sheets to the tension side in addition to external U-shaped CFRP sheets to restore the strength loss due to corrosion. Corroded beams with stirrups

were repaired by bonding longitudinal CFRP sheets to the tension side only. The test results showed that using externally bonded U-shaped CFRP sheets restored the ductility of corroded beams without stirrups and prevented bond failure at the steel concrete interface due to the absence of internal stirrups. In addition, combining U-shaped and longitudinal CFRP sheets enhanced the ultimate load by 37 % and the stiffness by 25 % in corroded beams without stirrups. For corroded beams with stirrups ductile failure was observed. Corroded beams with stirrups strengthened with CFRP sustained higher failure loads; however, the stiffness was unchanged.

**Keywords** Strengthening · Rehabilitation · Retrofitting · Corrosion · Transverse steel · Advanced composite materials · CFRP sheets

## 1 Introduction

The deterioration of reinforced concrete structures resulting from corrosion of steel reinforcement is a worldwide problem, and the cost of repairs is substantial. A common case of reinforcement corrosion is induced by the ingress of chloride ions ( $\text{Cl}^-$ ), water, and oxygen into uncontaminated concrete. Fresh concrete protects the steel reinforcement from corrosion by the formation of a passive layer in the highly alkaline ( $\text{pH} > 13$ ) environment of fresh

---

A. H. Al-Saidy (✉) · S. El-Gamal ·  
K. S. Al-Jabri · B. M. Waris  
Department of Civil and Architectural Engineering,  
Sultan Qaboos University, Muscat, Oman  
e-mail: alsaidy@squ.edu.om

H. Saadatmanesh  
Department of Civil Engineering and Engineering  
Mechanics, University of Arizona, Tucson, USA

concrete. However, this passive layer will be destroyed by  $\text{Cl}^-$  ions which initiate the corrosion process. While it is known that reinforcing steel provides strength and ductility only through bond and anchorage to the concrete, the effectiveness of such a bond mechanism can be reduced through deterioration of the steel, concrete or both. Numerous reported studies [1–7] suggest that loss in the structural performance of reinforced concrete members with corroded reinforcements are caused by three factors: losses in the effective cross-sectional area of concrete due to cracking in the cover concrete, losses in the mechanical performance of reinforcing bars due to the losses in their cross-sectional area and losses in the bond performance of concrete with reinforcements. Hence, the serviceability as well as the ultimate capacity of the damaged reinforced concrete member is affected.

The major factors that affect the bond between concrete and reinforcement in reinforced concrete are: concrete strength, concrete cover, bar spacing, bar geometry and surface conditions, and confinement [8]. Confinement can be either active by the reinforced concrete beam being in direct contact with a support or passive due to the presence of internal stirrups. Several researchers have studied the effect of confinement on the bond behaviour of steel in reinforced concrete members. It was concluded that transverse reinforcement improves the bond strength between the longitudinal reinforcement and the concrete [9, 10]. Fang et al. [11, 12] reported that for deformed bars without confinement, bond strength was very sensitive to corrosion levels and generally decreased with the increase in corrosion level. Bond strength decreased rapidly as the corrosion level increased; bond strength at 9 % corrosion level (9 % mass loss) was only one third of that of noncorroded specimens. For deformed bars with confinement, corrosion had no substantial influence on the bond strength. Al-Sulaimani et al. [13] studied the effect of corrosion and concrete cracking on the bond strength of reinforcing steel. In concentric pull-out tests of 10, 14, 20 mm bars embedded in 150 mm concrete cubes, bond strength increased by a maximum of 50, 33 and 55 % respectively at about 1 % mass loss. Beyond 1 % mass loss, bond strength decreased, dropping below the bond strength of the uncorroded bars only when the first crack were detected. Based on linear interpolations of the pull-out data, it was found that bond

strength was negligible for the 10, 14, and 20 mm bars at 6.5, 7.5 and 8.5 % mass loss respectively. It was concluded that the critical point in strength degradation occurs at the formation of cracks along the reinforcing bar. This confirms the conclusions of the study by Uomoto et al. [1]. The initial increase in bond strength of a corroded rebar was attributed to increased roughness provided by the firm layer of corrosion products. As the degree of corrosion increased and the longitudinal cracks were formed, the decrease in bond strength was attributed to severely deteriorated reinforcing bar ribs and reduced concrete confinement due to longitudinal crack widening.

The effect of corrosion of the longitudinal reinforcing steel on the strength and ductility of reinforced concrete beams is more critical if combined with corrosion of stirrups or if the beam is without stirrups. Researchers reported that the shear strength of members designed two to three decades ago was overestimated and the code conditions at that time for provisions of stirrups were not as stringent as codes today. As a result, a large number of structures in service are without stirrups, with minor margin of safety [14, 15]. A case of partial collapse of an overpass in 2006 in Quebec, Canada as a result of shear failure was reported by Jonson et al. [16]. It turned out that the collapsed portion of the overpass was a thick cantilever slab that was constructed without stirrups that lead to shear failure. In addition, the top reinforcement were not anchored at the ends due to detailing flaw. A study by Jeppsson and Thelander [17] found that shear strength decreases with loss of bond between longitudinal reinforcement and concrete. Xia et al. [18] examined the influence of reinforcing steel corrosion on the shear strength of reinforced concrete beams with different corrosion levels in both longitudinal reinforcing steel bars and stirrups. The study concluded that both the stiffness and shear strength of the beam decrease as the corrosion level increases. However, the decrease of the stiffness is insignificant when the applied load is relatively low. It is only when the applied load exceeds 20–30 % of its ultimate load, the stiffness loss caused due to the reinforcing steel corrosion becomes significant. Juarez et al. [19] reported that beam ductility was affected by levels of moderate and severe deterioration of stirrups, and this was evident due to the brittleness and sudden failure observed during beam testing. In a recent study,



Azam and Soudki [20] presented the behavior of reinforced concrete slender beams without stirrups and with corroded longitudinal reinforcement anchored at the end with standard 90° hooks. They found that the absence of stirrups combined with loss of bond along the longitudinal reinforcement due to corrosion changed the mode of failure from beam action to arch action. There was an increase in failure load and deflections compared to the control uncorroded beams. The findings by Azam and Soudki [20] are valid for properly anchored longitudinal reinforcement; but what if the corroded longitudinal reinforcement are not anchored. With such contradictory findings, more research is needed in this area.

Repair or strengthening with fiber reinforced polymers (FRP) has gained attention in recent years. It involves the external bonding of FRP sheets or plates to reinforced concrete beams and slabs, or confinement of reinforced concrete columns. FRP systems can also be used in areas with limited access where traditional techniques would be difficult to implement. Extensive research was done in the strengthening of concrete beams; however, limited number of work was directed towards strengthening of concrete elements damaged by corrosion of reinforcement. Available studies have shown that repair and strengthening of corrosion damaged reinforced concrete beams with externally bonded FRP sheets is efficient in restoring the strength of concrete members [21–26].

This paper presents the research findings of an experimental study involving damage due to chloride induced corrosion in the flexural reinforcement of concrete beams without shear reinforcement and concrete beams with minimum shear reinforcement. The main objective is to evaluate the effect of corrosion of longitudinal reinforcement without anchorage on the structural behavior and the effectiveness of carbon fiber reinforced polymers (CFRP) in repair of corroded beams.

## 2 Test program

### 2.1 Specimen details

The experimental program consisted of testing 12 rectangular reinforced concrete beams of 2.7 m long, 100 mm wide and 150 mm deep. The beams are divided into two groups. In Group A, a total of 7

reinforced concrete beams were tested as summarized in Table 1. The first group was constructed as reinforced concrete section without stirrups and reinforced by two straight 10-mm diameter bars tension reinforcement as shown in Fig. 1. Shear strength was calculated according to ACI 318 code [27] as per the shear strength equations shown in Table 1. Beam AC0 was a control beam with no corrosion, while beams AC5 and AC7.5 were subjected to accelerated corrosion with theoretical 5 and 7.5 % corrosion (mass loss in reinforcement). Beams ARU5 and ARU7.5 were corroded beams with corrosion of 5 and 7.5 %, respectively and then were repaired by applying six U-shaped CFRP sheets spaced 350 mm c/c approximately equivalent to the spacing of the stirrups used in beams of Group B. The remaining two beams, beams ASUL5 and ASUL7.5 were damaged with corrosion of 5 and 7.5 %; then were strengthened by bonding one layer of CFRP sheet along the tension side of the beam followed by adding U-shaped CFRP sheets.

The second group (Group B) consisted of 5 reinforced concrete beams with stirrups as summarized in Table 1. All beams were reinforced with two straight 10 mm diameter bottom bars (tensile reinforcement) and two 8 mm diameter top bars to hold the stirrups as shown in Fig. 2. The clear concrete cover was 20 mm on all sides of the cross section. For stirrups, 6-mm diameter epoxy coated plain bars spaced at 300 mm c/c were used within the shear span. The stirrups were epoxy coated to insure they will not get corroded during accelerated corrosion process of the tensile reinforcement. In Group B, Beam BC0 was a control beam with no corrosion, while beams BC5 and BC7.5 were subjected to accelerated corrosion with 5 and 7.5 % corrosion (mass loss in tensile reinforcement). Beams BS5 and BS7.5 were strengthened by applying CFRP sheet at the bottom of the beam only.

### 2.2 Material properties

Ordinary Portland cement was used for the concrete mix along with a maximum aggregate size of 10 mm. The concrete mix was proportioned by weight as follows, aggregate: sand: water: cement = 60: 67: 16: 25, with a water to cement ratio of 0.64. The concrete had an average 28-day compressive strength of  $35 \pm 1.5$  MPa. The average yield strength of the 10 mm diameter reinforcing bars was measured as

**Table 1** Details of test specimens

Beam designation	Theoretical mass loss (%)	Stirrups	CFRP U-strips	CFRP longitudinal sheet	$f'_c$ (MPa)	$f_y$ (MPa)	$\rho$	$V_n$ (kN)
AC0	0.0	–	–	–	35	420	0.013	11.9
AC5	5.0	–	–	–	35	420	0.013	11.9
AC7.5	7.5	–	–	–	35	420	0.013	11.9
ARU5	5.0	–	✓	–	35	420	0.013	11.9
ARU7.5	7.5	–	✓	–	35	420	0.013	11.9
ASUL 5	5.0	–	✓	✓	35	420	0.013	11.9
ASUL7.5	7.5	–	✓	✓	35	420	0.013	11.9
BC0	0.0	✓	–	–	35	420	0.013	17.6
BC5	5.0	✓	–	–	35	420	0.013	17.6
BC7.5	7.5	✓	–	–	35	420	0.013	17.6
BS5	5.0	✓	–	✓	35	420	0.013	17.6
BS7.5	7.5	✓	–	✓	35	420	0.013	17.6

$V_n = V_c + V_s$  ..... ACI - 318 [Ref.27]  
 $V_n = 2\sqrt{f'_c} b_w d + A_s f_y \frac{d}{s}$   
 $V_c =$  Shear strength provided by concrete  
 $V_s =$  Shear strength provided by stirrups

$f'_c =$  Concrete compressive strength  
 $f_y =$  Steel yield strength  
 $\rho = A_s/b.d$  (Reinforcement ratio)  
 $\rho_{min} = 0.003$  &  $\rho_{max} = 0.024$  (ACI-318 [Ref. 27])

420 MPa with Modulus of Elasticity of 200 GPa. The yield strength of the 6 mm diameter plain reinforcing stirrups was 250 MPa.

Unidirectional carbon fiber sheets were used for the bottom longitudinal sheets and the U-Shaped CFRP strips. The CFRP sheets had a thickness of 0.11 mm (dry fibers), tensile strength of 3800 MPa, Modulus of Elasticity of 240 GPa, and ultimate elongation of 1.55 % as indicated in the data sheets provided by the manufacturer. A two part epoxy was used to bond the CFRP sheet to the concrete surface. One coat of epoxy was first applied to the concrete surface, then the CFRP sheet was attached to the epoxy coated concrete and a second coat of epoxy was applied to the CFRP sheet. The composite laminate (fiber + epoxy) had an average thickness of 1 mm.

### 2.3 Preparing the specimens

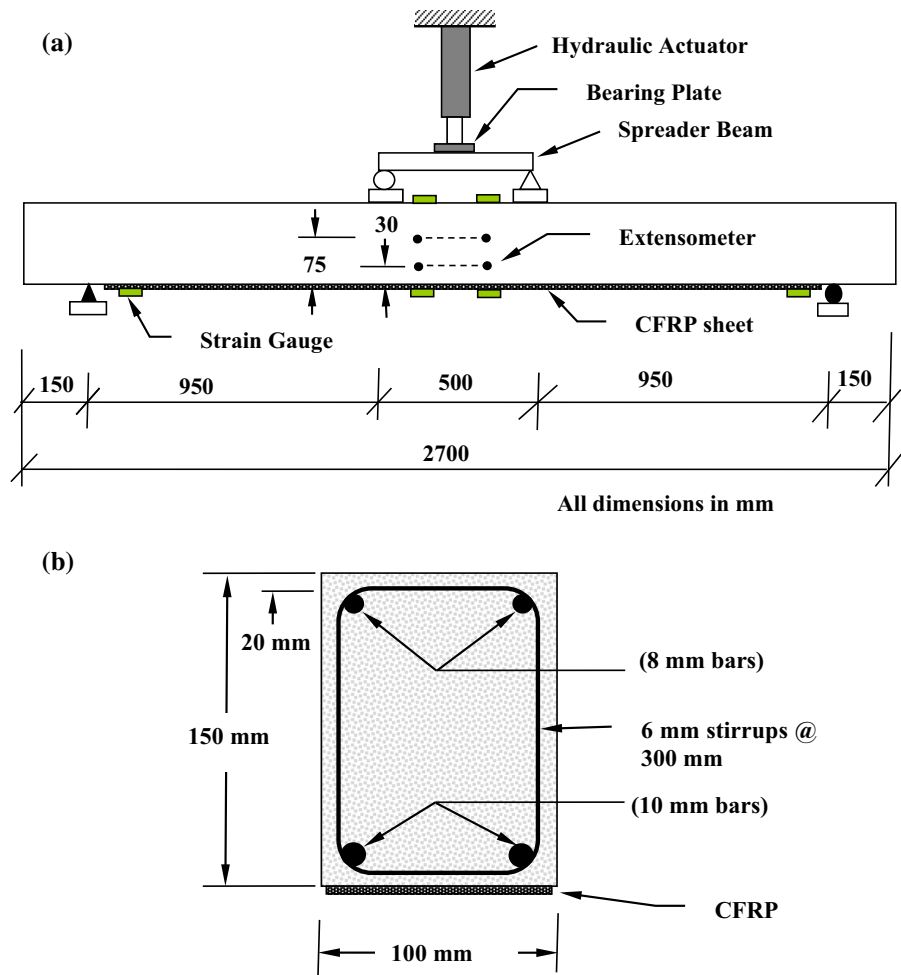
Casting of each beam was done in two layers; the first layer of concrete contained salt approximately 1 % by weight of cement in the mix which covered up to one third of the section height (above the tensile steel bars). This was done to simulate chloride ions ( $Cl^-$ ) contamination and to accelerate corrosion. The first

layer was compacted using a vibrator and then left for 30 min to partially set before the second layer of concrete was cast. The second layer of concrete was poured up to the top of the beam and compacted with a vibrator to insure no segregation takes place at the top of the first layer. No salt was used in the second layer. However, beams AC0 and BC0 were cast without the addition of salt to concrete as these beams were control specimens with no corrosion. After 28 days curing in room conditions at 25 °C temperature and 60 % humidity, the beams to be subjected to accelerated corrosion were placed inside a tank which has salted water with a concentration of about 3 % by weight of water (see Fig. 3). To induce corrosion in the reinforcement, the rebars were connected to a power (voltage) source where a current was applied to accelerate the corrosion process as shown in Fig. 3. Accelerated corrosion was carried out by impressing an electric current through the main longitudinal bottom reinforcing bars of about 488 mA, which corresponds to approximate current density of 281  $\mu A/cm^2$ . This current density was obtained by dividing the total impressed current by the surface area of the steel reinforcement that is in the salt contaminated concrete (specimen's bottom third). The





**Fig. 2** a Test setup for beams with stirrups, b cross section details



theoretical 5 % corrosion (or 5 % mass loss in reinforcing bar) it was found that the time required to produce this mass loss was 14 days of continuous application of 488 mA current in each beam (see [Appendix](#)).

Following the experimental tests of the beams, the actual mass loss due to steel reinforcement corrosion was measured using bars that were extracted from the corroded beams (see [Fig. 4](#)). The procedure given in ASTM standard G1, designation C.3.5, was used for the mass loss analysis [31]. Six bar coupons 250 mm in length were taken from the corroded bottom bars of each corroded beam. The coupons were taken at random from both of the corroded bars in each beam since the corrosion was assumed to be uniform along the entire length of the beam. Bar coupons from the control beams were used as a reference. [Table 2](#)

summarizes the mass loss results. Faraday's law tends to overestimate the mass loss for medium to high corrosion rates (5 and 7.5 %). Al-Hammoud et al. [32] reported similar finding and one explanation is that after sometime of the acceleration process, the corrosion products built up around the bar and filled the cracks, thus reducing the concentration of oxygen and water around the bar, which slows down the corrosion rate.

Following the accelerated corrosion phase, the beams were left for 2 days to dry. The beams were then repaired with CFRP and were left for a week for the CFRP to cure under room temperature. Bonding of the CFRP to the concrete was achieved by using epoxy adhesive. Prior to applying the epoxy and CFRP, the surface of the concrete was prepared by grinding the concrete with a disc grinder in the area to receive the CFRP.



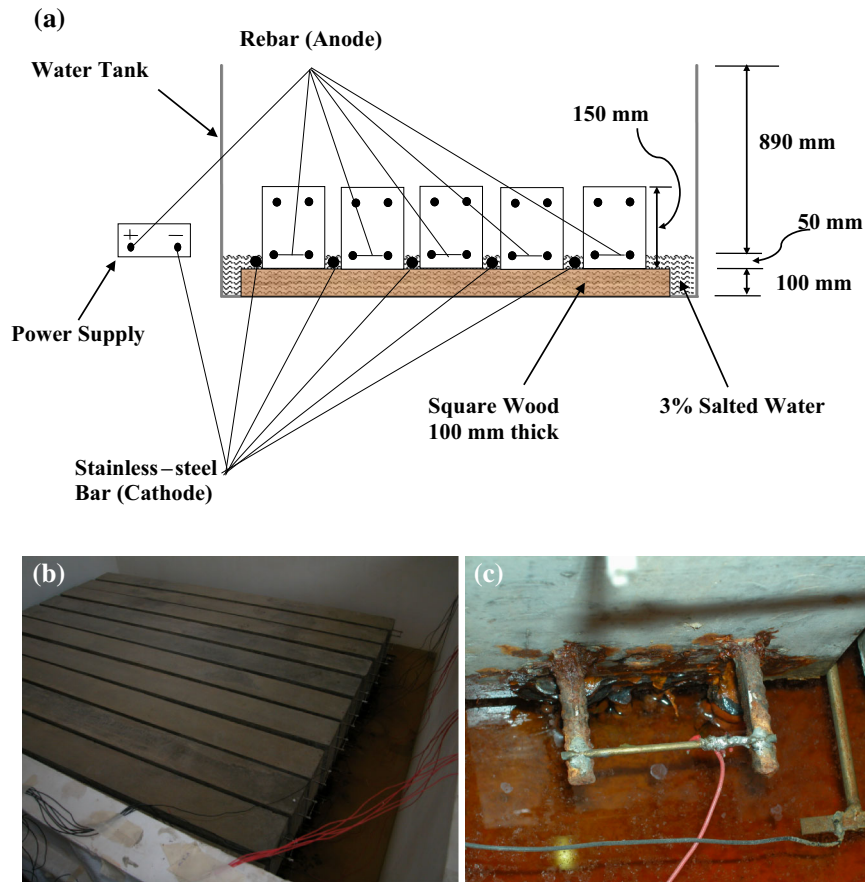


**Fig. 3** a Schematic of accelerated corrosion setup; b Beams in the conditioning tank; c Connection of the tension reinforcement (anode) and the stainless steel bar (cathode)



**Fig. 4** Extracting the corroded bars after the test for evaluation of the actual mass loss

## 2.4 Test setup and instrumentation

All specimens were loaded in four-point loading (see Figs. 1 and 2). The load was applied using a 250 kN hydraulic actuator through a spreader steel beam to the specimen. Four linear variable displacement transducers (LVDTs) with a range capacity of 100 mm were used to measure the quarter lines and mid-span deflections of the beam during testing; two electrical strain gauges (60 mm long) at the top of the beam to measure the concrete strain and two extensometer of gauge length of 200 mm and range capacity of  $\pm 5$  mm was used to measure the side strain of concrete. For beams strengthened with longitudinal CFRP sheets four electrical strain gauges (6 mm long) were installed along the centerline of CFRP sheet.

**Table 2** Theoretical and experimental mass loss

Beam designation	Theoretical mass loss (%)	Experimental mass loss (%)
AC5	5.0	4.2
AC7.5	7.5	7.0
ARU5	5.0	4.7
ARU7.5	7.5	6.7
ASUL 5	5.0	5.2
ASUL7.5	7.5	6.5
BC5	5.0	3.8
BC7.5	7.5	6.4
BS5	5.0	5.1
BS7.5	7.5	6.2

Strain gauges were also installed at the mid-height of the U-shaped CFRP sheets along the vertical direction (i.e. transverse to the beam axis). All beams were tested to failure using displacement control with a rate of 0.3 mm/min.

### 3 Test results and discussion

#### 3.1 Effect of corrosion

The beams subjected to accelerated corrosion were cracked along the beam parallel to the steel reinforcement. Beams without stirrups, the corrosion cracks were mainly on the side of the beams, while beams with stirrups the cracks were on the soffit of the beam and in some cases on the sides of the beam as well.

The test results of all tested beams are summarized in Table 3. The load versus mid-span deflections are shown in Fig. 5. Figure 5a shows that the behavior of beam AC0 (without stirrups and with 0 % corrosion) is of a typical under-reinforced beam exhibiting large deformation beyond the yield point before it failed by crushing of concrete. However, corroded beams without stirrups (AC5 and AC7.5) failed in a brittle manner due to debonding between reinforcement and concrete (see Fig. 6). The beam literally split into two pieces longitudinally at the level of the corroded rebars. The maximum deflections at failure were 66, 23 and 25 mm for beams AC0, AC5 and AC7.5, respectively. The ultimate deflection was reduced due to corrosion by approximately 63 % compared to the control uncorroded beam (beam AC0). On the other hand, beams with stirrups (Fig. 5b) lost some strength

due to corrosion, but failed in a ductile manner. The maximum deflections were 43, 40 and 32 mm for beams BC0, BC5 and BC7.5, respectively. This indicates a reduction in deflection of 1 and 25 % in beams BC5 and BC7.5 relative to the control uncorroded beam (beam BC0). All beams with stirrups failed by crushing of concrete after steel has yielded.

#### 3.2 Effect of stirrups on load deflection behavior

The effect of stirrups on the load deflection behavior of the control and corroded beams is presented in Fig. 7. Beams with stirrups showed higher stiffness and resisted slightly higher loads. Stiffness is approximated as the slope of the load deflection curve in the elastic range before yielding. In other words, stiffness is defined as the ratio of the yielding load,  $P_y$ , divided by the yielding deflection,  $D_y$ . The control beam without stirrups failed at a load of 15.8 kN and a deflection of 66 mm, while the control beam with stirrups failed at a load of 17 kN and a deflection of 43 mm. The control beams with/without stirrups showed a ductile behavior. However, the presence of stirrups increased the stiffness by approximately 17 %. The effect of stirrups is more prominent in the corroded beams as shown in Fig. 7b. The corroded beam without stirrups failed at a load of 12 kN and a deflection of 25 mm, while the corroded beam with stirrups failed at a load of 14 kN and a deflection of 32 mm. It is also noted that the existence of stirrups increased the deflection at ultimate load by 22 % and stiffness by 32 % of the corroded beams. The increase in stiffness was mainly due to the confinement provided by the stirrups. When corrosion takes





**Table 3** Summary of test results

Specimen	Experimental						Mode of failure
	$P_y$ (kN)	$D_y$ (mm)	$P_u$ (kN)	$D_u$ (mm)	$V_u$ (kN)	$V_n$ (kN)	
AC0	14.2	20	15.8	66	7.9	11.9	CC
AC5	14.4	18	14.6	23	7.3	11.9	BF
ARU5	13.2	20	14.8	56	7.4	11.9	CC
ASUL 5	17.2	19.3	21.8	60	10.9	11.9	CC
AC7.5	12	22	12	25	6	11.9	BF
ARU7.5	13	22	14	48	7.0	11.9	CC
ASUL7.5	14	16	14	16	7.0	11.9	DU + BF + S
BC0	15.5	18	17	43	8.5	17.6	CC
BC5	14	16	16.3	40	8.15	17.6	CC
BS5	16	20	20	48	10	17.6	RT
BC7.5	13	16	14	32	7	17.6	CC
BS7.5	16	18	20	46	10	17.6	DB + RT

$P_y$  = Yielding load  
 $P_u$  = Ultimate load  
 $D_y$  = Yielding deflection  
 $D_u$  = Max. deflection  
 $V_u$  = Ultimate shear force =  $P_u/2$   
 $V_n$  = Nominal shear strength(analytical)

CC = Concrete crushing  
 BF = Bond failure at steel concrete interface  
 S = Shear  
 DU = Debonding of U-shaped strip  
 RT = CFRP rupture  
 DB = Debonding of CFRP longitudinal sheet

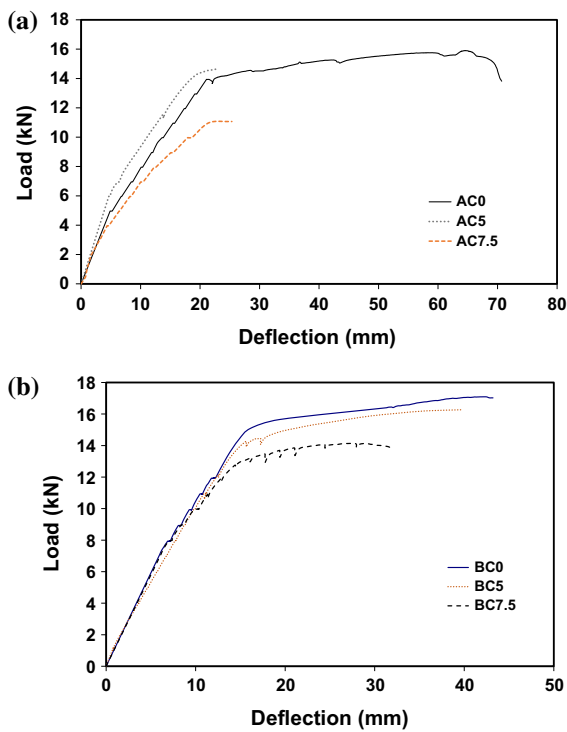


**Fig. 5** Effect of corrosion **a** Group A beams, without stirrups, **b** Group B beams, with stirrups



**Fig. 6** Bond failure of beam AC5&AC7.5

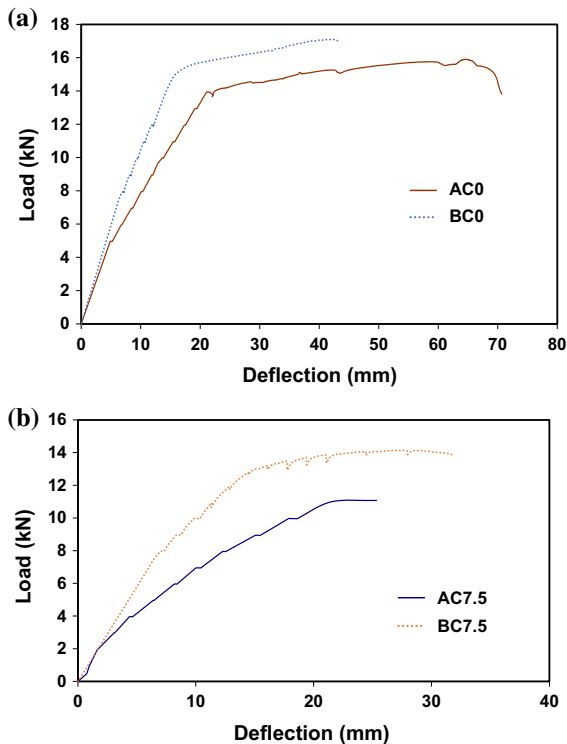


**Fig. 7** Effect of stirrups on beams. **a** control **b** corroded

place in beams without stirrups, the bond is affected and only depends on the interlocking forces between the ribs of the bars and the surrounding concrete keys [33]. Corroded beams without stirrups seems to lose some stiffness due to formation of transverse as well as longitudinal cracks along the steel bars. This can be attributed to the weakened bond along the interface of the steel bar and the concrete that renders the beam to behave in a similar way as partially composite beam and hence larger deformations or loss of stiffness compared to beams with stirrups that maintain the composite action between concrete and flexural steel. The presence of stirrups provides the confinement needed such that the flexural steel will act compositely with concrete in compression as one unit.

### 3.3 Effect of U-shaped CFRP strips repair

Attaching U-shaped CFRP strips on corroded beams without stirrups changed the mode of failure of the repaired beams. Figure 8 illustrates the effect of U-shaped CFRP repair on the corroded beams without

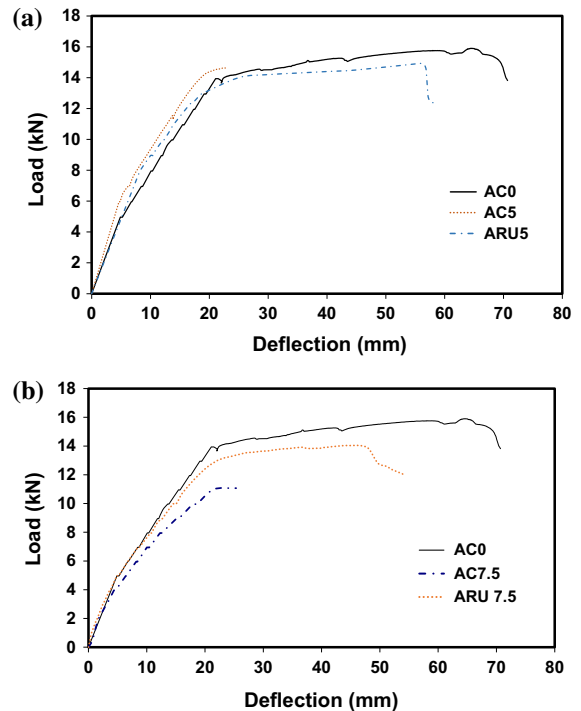


**Fig. 8** Effect of CFRP U-wrap strips on beams without stirrups. **a** Beams with 5 % corrosion. **b** Beams with 7.5 % corrosion

stirrups. Adding U-shaped sheets improved the strength by attaining higher ultimate load and improved ductility indicated by higher maximum deflection at failure. This is observed from the response of beams ARU5 and ARU7.5 which failed by crushing of concrete compared to a brittle failure observed in beams AC5 and AC7.5. The maximum deflections were increased by 59 % and by 48 % in beams ARU5 and ARU7.5 compared to beams AC5 and AC7.5, respectively due to the CFRP repair. Figure 9 shows locations of U-shaped CFRP sheets and corresponding locations of strain gauges. Strain was measured along the U-shaped CFRP sheet (i.e. transverse the beam axis). The change of strain in the U-shaped CFRP sheets in beam ARU5 is shown in Fig. 10; strain in FRP2 is higher than in FRP1 since FRP2 sheet is located in the shear span where stirrups are needed most. FRP2 sheet provided the anchoring force as observed from the increase in the strain at higher applied loads indicating the effectiveness of externally attached CFRP U-shaped strips. FRP3 was located next to the support and as such was subjected to minor strain since the deformations are small near

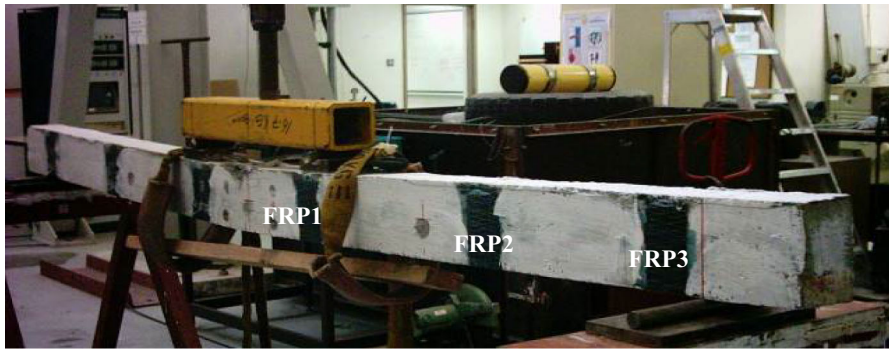


**Fig. 9** Locations of strain gauges in the U-shaped CFRP sheets

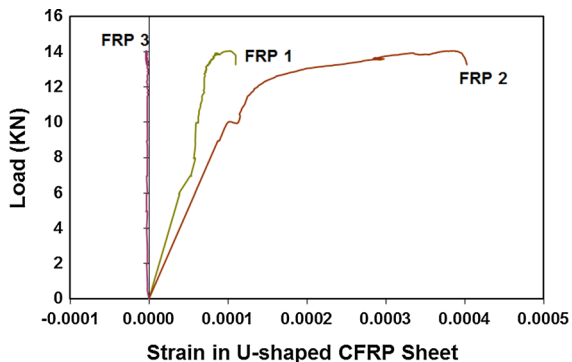


**Fig. 10** Strain in the U-shaped CFRP sheets in beam ARU5

the support and also the compressive force provided by the support reaction provided an anchoring action which reduced the stress from the U-shaped CFRP sheet near the supports.

### 3.4 Effect of CFRP sheet strengthening

The load deflection curves for strengthened beams without stirrups are shown in Fig. 11a, b, while strengthened beams with stirrups results are shown in Fig. 11c, d. Adding CFRP sheet and U-shaped sheets to strengthened corroded beams without stirrups increased both ultimate load and stiffness of the repaired beam. The ultimate load of beam ASUL5 was increased by about 37 and 47 % compared to the uncorroded control beam AC0 and the corroded beam ARU5, respectively. Adding the CFRP sheet delayed the cracking of the concrete and enhanced the stiffness of the beam as may be

observed from the load vs. deflection curve shown in Fig. 11a. An increase in stiffness by about 25 % in beam ASUL5 compared to the control uncorroded beam AC0. Beam ASUL5 failed by crushing of concrete after a large deflection beyond the yielding load.

Following the accelerated corrosion phase, Beam ASUL7.5 was severely cracked along the reinforcement on the side where the rebars were connected to the voltage source. It is believed that more moisture penetrated the beam through the cracks from the partially immersed bar ends. This produced higher concentration of corrosion on one side of the beam. This beam failed prematurely in a brittle manner as one of U-shaped sheets debonded, the crack along the beam opened up and finally failed in bond-shear mode as shown in Fig. 12. Even though beam ASUL7.5 failed prematurely, it is observed that within the elastic range the stiffness was improved compared to beams AC0 and ARU7.5.

Strengthened beams with stirrups (Fig. 11c, d) attained higher ultimate loads compared to the corroded and control beams, but the stiffness was almost unchanged. Beam BS5 strengthened by CFRP sheet at the tension side was able to sustain load higher than beam BC0 and beam BC5 by 3 and 9.5 %, respectively. The yield load was also higher in the strengthened beam BS5 than both control beams (BC0 & BC5). Beam BS5 failed by CFRP rupture at mid-span which was mainly due to the opening of the horizontal corrosion crack that pushed the cover concrete against the CFRP sheet creating concentration of stresses on the CFRP

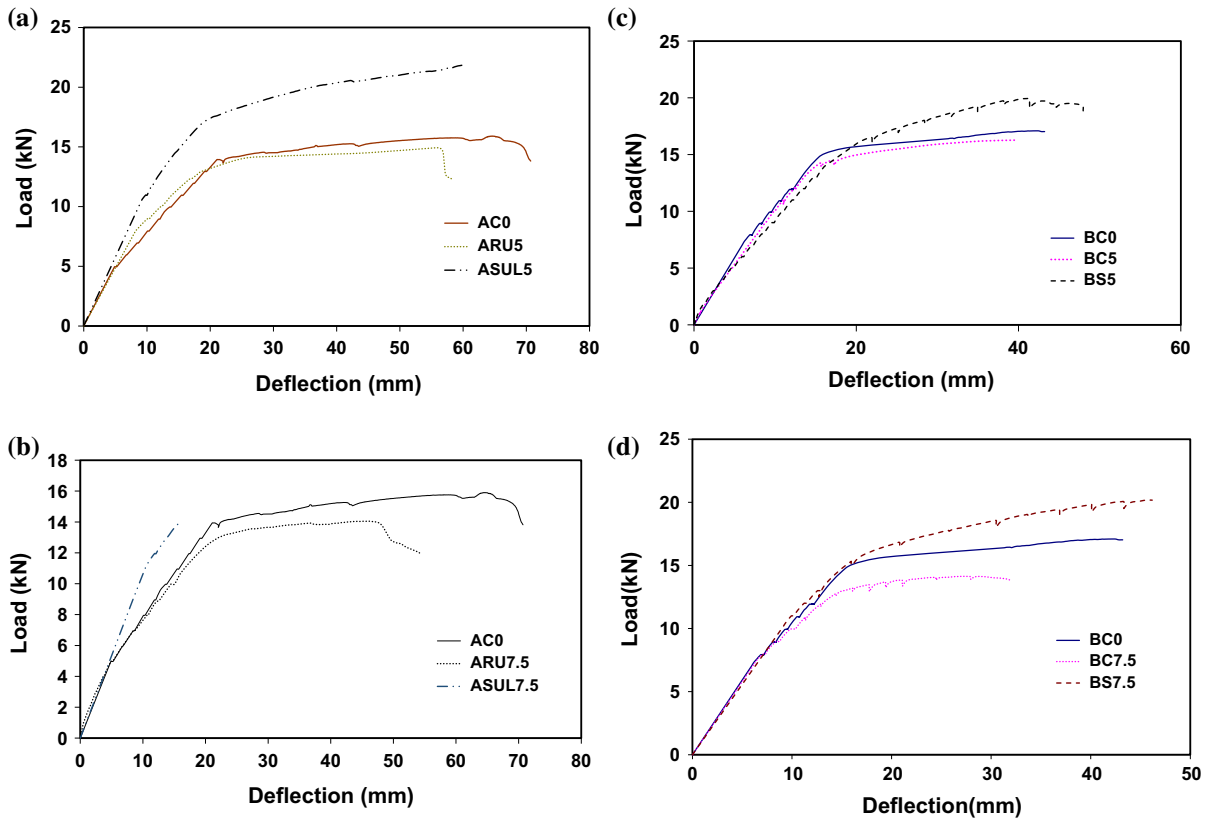


Fig. 11 Effect of CFRP sheet strengthening: a, b beams without stirrups; c, d beams with stirrups

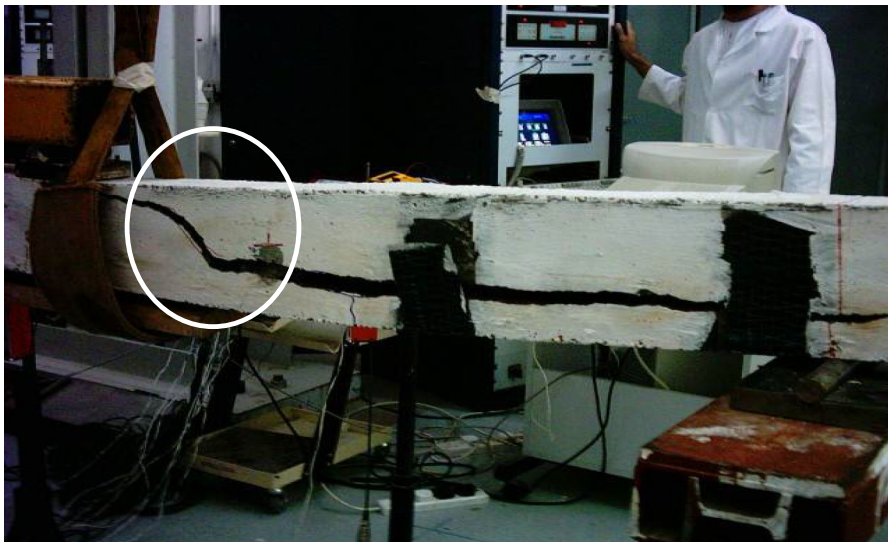


Fig. 12 Bond-shear failure of beam ASUL7.5



**Fig. 13** Separation of concrete cover and CFRP in beam BS7.5

sheets. The ultimate load of beam BS7.5 reached 20 kN which is 18 and 43 % higher than ultimate loads of beams BC0 and BC7.5, respectively. Failure of beam BS7.5 was initiated by the separation of concrete cover where flexural cracks (vertical) crossed the corrosion cracks (horizontal) along the reinforcing bars. The CFRP sheet was pushed away from the beam surface (partial debonding), but finally failed by rupture at the tip of the cracked area (see Fig. 13).

#### 4 Conclusions

This study presented the results of an experimental investigation of the structural behavior of reinforced concrete beams with corroded longitudinal reinforcement not anchored at their ends. Two groups of beams were tested; one group had corroded longitudinal reinforcement without stirrups and the second group consisted of beams with corroded longitudinal reinforcement with stirrups. Based on the experimental results, the following conclusions are drawn:

- Corroded beams without stirrups failed in a brittle manner with drop in maximum deflection at failure

of approximately 60 % compared to the uncorroded beam.

- Corroded beams with stirrups lost some strength, but failed in ductile manner. The reduction in maximum deflection due corrosion ranged between 1 and 25 % for 5 % mass loss and 7.5 % mass loss, respectively compared to the uncorroded beam.
- Corroded beams without stirrups repaired by U-shape CFRP strips effectively confined the corroded beams and changed the mode of failure to a ductile failure. The maximum deflection of repaired beams increased by 59 % in beam with 5 % mass loss and by 48 % in beam with 7.5 % mass loss compared to the unrepaired corroded beams with the same mass loss.
- Strengthening corroded beams without stirrups with CFRP sheet and U-shaped CFRP strips enhanced the ultimate load by 37 % and the stiffness by 25 % for beams with 5 % corrosion.
- Strengthening corroded beams with stirrups increased the ultimate load in the range of 9–43 %, but no change in the beam stiffness.

#### Appendix

See Table 4.



**Table 4** Impressed current calculations

## Main rebar

Length of exposed tensile steel in concrete = 2760.00 (mm)

Diameter of rebar = 10.00 (mm)

Cross-sectional area of rebar = 78.57 (mm<sup>2</sup>)

No. of rebars = 2.00

Volume of exposed tensile steel = 433714.29 (mm<sup>3</sup>) = 0.424 × 10<sup>-3</sup>(m<sup>3</sup>)

Surface area of exposed steel = 173485.71 (mm<sup>2</sup>) = 1735 (cm<sup>2</sup>)

Density of steel = 7860.00 (kg/m<sup>3</sup>)

Mass of steel in salt contaminated concrete = 7860 kg/m<sup>3</sup> × 0.424 × 10<sup>-3</sup> m<sup>3</sup> = 3408.99 (g)

Percentage of mass loss = 5 %

Mass loss = (5/100) × 3334.89 g = 170.45 (g)

## Current

Knowing that 1 Amp-h consume 1.04 g of Iron (Philip [30])

Required Amp-h to cause mass loss = 170.45 g × 1Amp-h/1.04 g = 163.89 Amp-h

Duration of exposure in no. of weeks = 2 weeks

Applied current for one beam = 163.89 Amp-h/(2 × 7 × 24 h) = 487.78 (mA)

Current density = (487.78 mA/1735 cm<sup>2</sup>) × 10<sup>3</sup> = 281.16 (μA/cm<sup>2</sup>)

## References

- Umoto T, Tsuji K, Kakizawa T (1984) Deterioration mechanism of concrete structures caused by corrosion of reinforcing bars. *Tran Jpn Concr Inst* 6:163–177
- Almusallam A, Al-Gahtani A, Aziz A, Dakhil F, Rasheeduzzafar (1996) Effect of reinforcement corrosion on flexural behavior of concrete slabs. *J Mater Civil Eng* 8:123–127
- Cabrera JG (1996) Deterioration of concrete due to reinforcement steel corrosion. *Cem Concr Compos* 18:47–59
- Baweja D, Ropert H, Sirivivatnanan V (1999) Chloride-induced steel corrosion in concrete. *ACI Mater J* 96(3):306–313
- Morinaga S (1996) Remaining life of reinforced concrete structures after corrosion cracking. *Durab Build Mater* 17:127–136
- Okada K, Kobayashi K, Miyagawa T (1988) Influence of longitudinal cracking due to reinforcement corrosion on characteristics of reinforced concrete members. *ACI Struct J* 85:134–140
- Katayama S, Maruyama K, Kimura T (1995) Flexural behaviour of RC beams with corrosion of steel bars. The 49th annual meeting of japan cement association, Japan cement association, Tokyo, pp. 880–885
- ACI Committee 408 ACI 408R-03 (2003) Bond and development of straight reinforcing bars in tension. Farmington Hills (MI): American Concrete Institute, p. 49
- Zuo J, Darwin D (2000) Splice strength of conventional and high relative rib area bars in normal and high-strength concrete. *ACI Struct J* 97:630–641
- Al-Hammoud R, Soudki K, Topper TH (2013) Confinement effect on the bond behaviour of beams under static and repeated loading. *Constr Build Mater* 40:934–943
- Fang C, Lundgren K, Chen L, Zhu C (2004) Corrosion influence on bond in reinforced concrete. *Cem Concr Res* 34:2159–2167
- Fang C, Lundgren K, Plos M, Gylltoft K (2006) Bond behaviour of corroded reinforcing steel bars in concrete. *Cem Concr Res* 36:1931–1938
- Al-Sulaimani GJ, Kaleemullah M, Basunbul IA, Rasheeduzzafar (1990) Influence of corrosion and cracking on bond behavior and strength of reinforced concrete slab. *ACI Struct J* 87(2):220–231
- Sherwood EG, Lubell AS, Bentz EC, Collins MP (2006) One way shear strength of thick slabs and wide beams. *ACI Struct J* 103(6):180–190
- Sneed LH (2007) Influence of member depth on shear strength of concrete beams. Ph.D. thesis, Purdue University, West Lafayette
- Johnson PM, Couture A, Nicolet R (2007) Commission of inquiry into the collapse of a portion of the de la Concorde overpass. Final report, Government of Quebec. ([http://www.cevc.gouv.qc.ca/UserFiles/File/Rapport/report\\_eng.pdf](http://www.cevc.gouv.qc.ca/UserFiles/File/Rapport/report_eng.pdf)). Accessed March 2014)
- Jeppsson J, Thelandersson S (2003) Behavior of reinforced concrete beams with loss of bond at longitudinal reinforcement. *J Struct Eng* 129(10):1376–1383
- Xia J, Jin W, Li L (2011) Shear performance of reinforced concrete beams with corroded stirrups in chloride environment. *Corros Sci* 53:1794–1805
- Juarez CA, Guevaraa B, Fajardo G, Castro-Borges P (2011) Ultimate and nominal shear strength in reinforced concrete beams deteriorated by corrosion. *Eng Struct* 33:3189–3196
- Azam R, Soudki K (2013) Structural behavior of shear-critical RC slender beams with corroded properly anchored longitudinal steel reinforcement. *J Struct Eng* 139(12):04013011





21. Bonacci JF, Maaleej M (2000) Externally bonded fiber reinforcement polymer for rehabilitation of corrosion damaged concrete beams. *ACI Struct J* 97:703–711
22. Soudki K, Sherwood T (2000) Behaviour of reinforced concrete beams strengthened with carbon fiber reinforced polymer laminates subjected to corrosion damage. *Can J Civ Eng* 27:1005–1010
23. Kutarba MP, Brown JR, Hamilton HR. Repair of corrosion damaged concrete beams with carbon fiber-reinforced polymer composites. *Proceedings of COMPOSITES 2004*, Tampa
24. Soudki K, Rteil A, Al-Hammoud R, Topper T (2007) Fatigue strength of fibre-reinforced-polymer-repaired beams subjected to mild corrosion. *Can J Civ Eng* 34(3):414–421
25. Al-Saidy AH, Al-Harthy AS, Al-Jabri KS, Abdul-Halim M, Al-Shidi NM (2010) Structural performance of corroded RC beams repaired with CFRP sheets. *Compos Struct* 92:1931–1938
26. Xie JH, Hub RL (2012) Experimental study on rehabilitation of corrosion-damaged reinforced concrete beams with carbon fiber reinforced polymer. *Constr Build Mater* 38:708–716
27. ACI Committee 318 (2008) Building code requirements for structural concrete. (ACI 318-08) and Commentary (ACI 318R-08), Farmington Hills (MI), American Concrete Institute
28. Jones DA (1992) Principles and prevention of corrosion. MacMillan Publishing Company, New York
29. Roberge PR (1999) Handbook of corrosion engineering. McGraw-Hill, New York
30. Philips JMP (1991) The effect of corrosion on the structural performance of new and repaired one-way slabs. PhD Thesis, University of Toronto, Toronto
31. ASTM, G1 (2011) Standard practice for preparing, cleaning, and evaluating corrosion test specimens. West Conshohocken
32. Al-Hammoud R, Soudki K, Topper T (2011) Fatigue flexural behavior of corroded reinforced concrete beams repaired with CFRP sheets. *J Compos Constr* 15(1):42–51
33. Wang W, Liu X (2004) Modeling bond strength of corroded reinforcement without stirrups. *Cem Concr Res* 34:1331–1339